EXPERIMENTS AND COMPUTATIONS OF A LOOSELY SUPPORTED TUBE UNDER TWO-PHASE BUFFETING AND FLUID-ELASTIC COUPLING FORCES

X.Delaune[1], J.Antunes[2], P.Piteau[1], L.Borsoi[1]
[1]Commissariat à l'Energie Atomique et aux Energies Alternatives, Laboratoire d'Études de Dynamique, CEA,DEN,DM2S,SEMT,DYN, Saclay, France
[2]Instituto Tecnologico e Nuclear, Applied Dynamics Laboratory, ITN,ADL, Sacavem, Portugal
E-mail of corresponding author: xavier.delaune@cea.fr

ABSTRACT

In a recent paper we addressed the problem of predicting the nonlinear vibro-impact responses of loosely supported heat-exchanger tubes subjected to single-phase turbulence and fluid-elastic coupling forces from transverse flows. Here, we extend that previous work to two-phase flows, by presenting nonlinear time-domain predictive computations, as well as validation experiments, of the vibro-impacting dynamical tube responses, when subjected to the combined action of two-phase random buffeting excitation and fluid-elastic coupling forces. Emphasis is on the fluid-elastic modeling within a time-domain nonlinear framework, as well as on the stabilizing effect of impacts on the fluid-elastic coupling forces. Computations of the vibro-impacting regimes of a flow-excited cantilever test tube, within a rigid 3x5 square bundle, are based on the experimentally identified two-phase fluid-elastic coupling force coefficients and random excitation spectra, as a function of the homogeneous flow velocity, for a void fraction of 85 %. Computations are then compared with the experimental vibratory responses, enabling a satisfying preliminary validation of the modeling approach for two-phase flows.

INTRODUCTION

Heat-exchanger tube bundles are subjected to fluid-elastic coupling forces, which depend on the bundle geometry, fluid nature – single-phase or two-phase – and on the fluid velocity. Reliable modeling of such coupling forces is very difficult, therefore several authors since the pioneering work of Tanaka & Takahara [1] have attempted to measure the fluid-elastic linearized stiffness and damping coefficients as a function of the flow reduced velocity (or reduced frequency), for specific fluid mixtures and bundle geometries, in order to link the dynamical behavior of the flow-coupled tube bundle with simpler stability criteria such as provided by Connors [2] and many others since. When looking at the gap-supported tubes of real-life components, time-domain nonlinear computing methods have been developed by several research groups for the predictive analysis of vibro-impacting flow-excited tubes. As far as fluid-elastic forces are concerned, the first attempt to include them in the computations – along with the ever-present turbulent excitation – was achieved by Axisa et al. [3], who used a flow velocity-dependent negative damping coefficient on the linearly unstable mode, deduced from Connors formulation. This pioneering approach was followed by others, along similar lines – see Fricker [4], for instance, who additionally corrected the computation of the fluid-elastic coupling effect by using an estimate of the actual response frequency instead of the modal frequency of the unstable mode. Since then, others have tackled this problem in a more sophisticated manner, by directly incorporating in their computer programs models of the fluid-elastic coupling forces [5-8].

Nevertheless, it is still debatable how realistic are the strongly nonlinear and unsteady vibro-impact regimes produced by computations which stem from fluid-elastic coefficients obtained under linear and steady conditions. Furthermore, it is well known that, when gap-supported tubes become linearly unstable, impacting produces an increase of the actual tube response frequencies, which somehow tend to re-stabilize the system. Because of these difficulties, there is urgency in validating. We believe that carefully controlled experiments of gap supported tubes subjected to fluid-elastic coupling forces are needed, in view of validating the current computational approaches for such systems, as well as to increase our physical understanding of the stabilizing mechanisms provided by the impact dynamics.

Therefore, based on the active vibration control method proposed by Caillaud et al. [9], new experiments were recently performed at CEA-Saclay on the same experimental rig, consisting on a flexible tube (vibrating along the lift direction) inserted in a rigid square bundle [10]. First, the linearized fluid-elastic coupling coefficients, as well as the turbulence excitation from single-phase flow, were identified for a significant range of reduced velocity, in water cross-flow. Then, nonlinear experiments were performed under the same conditions after installing an instrumented loose support in the rig, from which both the tube responses and the impact forces were measured.

These experimental results were compared with the linear and vibro-impact numerically simulated responses obtained from a time-domain computer program, where the experimentally identified linear fluid-elastic coupling coefficients were implemented. A delicate aspect of such implementation is the real-time estimation of a representative instantaneous response frequency of the vibro-impacting tube, which is needed because the coupling coefficients depend on the "instantaneous" reduced frequency. For single-phase flows the results obtained using the developed methodology were quite satisfactory [10].

In this paper we now present the first results obtained by extending our previous work to two-phase flows. Theoretical computations of the vibro-impacting regimes of a flow-excited cantilever test tube, within a rigid 3x5 square bundle, are based on the experimentally identified two-phase fluid-elastic coupling force coefficients and random excitation spectra, as a function of the homogeneous flow velocity, for a void fraction of 85 %, which is a typical value in the upper region of steam generators. Details on the following aspects are reported in the paper: (1) Numerical modeling of the buffeting and fluid-elastic coupling forces for performing the time-domain computations; (2) Experimental identification of the fluid-elastic coupling coefficients and random excitation spectrum; (3) Computations and experiments of vibro-impacting responses under the combined action of the buffeting excitation and fluid-elastic coupling; and (4) Energy aspects of the vibro-impacting fluid-elastically coupled tube responses, which highlight the nonlinear stabilization of fluid-elastically unstable tubes.

NUMERICAL MODELING OF THE FLOW-EXCITED GAP-SUPPORTED TUBE

Time-Domain Computation of the Nonlinear Dynamics

As discussed in [3], the simple Bernoulli–Euler theory for flexural vibrations proved to be adequate for impact identification. Therefore, assuming a viscous damping model, the small-amplitude flexural response of a tube with constant cross-sectional properties is described by the differential equation:

$$\rho A \frac{\partial^2 Y}{\partial t^2} + \eta \frac{\partial Y}{\partial t} + EI \frac{\partial^4 Y}{\partial x^4} = f(x,t) = f_F(x,t) + f_T(x,t) + f_C(x,t) \tag{1}$$

where $f(x,t)$ is the total external excitation field and $Y(x,t)$ is the tube transverse flexural response, E is Young's modulus and ρ is the mass density of the tube, A is the area and I is the moment of inertia of the cross-section, while η is a viscous dissipation coefficient. The total excitation field in equation (1) stems from the fluid-elastic coupling forces $f_F(x,t)$, the turbulence forces $f_T(x,t)$ and the contact/impact forces $f_C(x,t) = \sum_C F_C(t)\,\delta(x - x_C)$ located at the loose supports x_C. As amply discussed by Axisa et al. [3] and Antunes et al. [11], the vibro-impact nonlinear computations under flow excitation may be performed in an effective manner by projecting equation (1) on the tube unconstrained modes $\varphi_n(x)$. Then, the following discretized modal equations are obtained [10]:

$$\left[\mathcal{M}_S\right]\left\{\ddot{Q}\right\} + \left[\mathcal{D}_S\right]\left\{\dot{Q}\right\} + \left[\mathcal{K}_S\right]\left\{Q\right\} = \left\{\mathcal{F}^F(t)\right\} + \left\{\mathcal{F}^T(t)\right\} + \left\{\mathcal{F}^C(t)\right\} \tag{2}$$

in terms of the vector of modal amplitudes $q_n(t)$ and its derivatives. The modal matrices of the left hand side of equation (2) are built from the modal masses m_n, frequencies ω_n and damping values ζ_n, with $n = 1, 2, ..., N$.

The total modal forces $F_n(t)$ in the vectors of right hand side of equation (2) are computed from the modal projections of the fluid-elastic, turbulence and contact/impact terms :

$$F_n^F(t) = \int_0^L f_F(x,t)\varphi_n(x)dx \quad ; \quad F_n^T(t) = \int_0^L f_T(x,t)\varphi_n(x)dx \quad ; \quad F_n^C(t) = \int_0^L \left(\sum_C F_C(t)\delta(x - x_C)\right)\varphi_n(x)dx = \sum_C F_C(t)\varphi_n(x_C) \tag{3}$$

where L is the tube length. The physical motions may be computed from the modal responses at any time and location, by modal superposition. The computational truncation index N of the modal basis is chosen accounting for the frequency ranges excited by the various sources of excitation.

Fluid-elastic Coupling Forces

In their recent work, Hassan & Hayder [8] developed a direct implementation of the Lever and Weaver [12] model to compute the fluid-elastic coupling forces, which does not require the knowledge of the instantaneous tube response frequency. However, the most common approach – and the only available if one wishes to use experimentally identified force data – is to express the linearized fluid-elastic forces $f_F(x,t)$ in terms of coupling coefficients M_F, D_F and K_F, which in general depend on V_R. Then, the fluid-elastic force reads:

$$f_F(x,t) = -M_F\ddot{Y}(x,t) - D_F\left(V_R(x,t)\right)\dot{Y}(x,t) - K_F\left(V_R(x,t)\right)Y(x,t) \tag{4}$$

where only the fluid inertia coupling coefficient does not depend on the reduced flow velocity $V_R(x,t) = V(x)\big/\left[\overline{f}_r(x,t)D\right]$. Here, $\overline{f}_r(x,t)$ is an estimate of the "instantaneous" local response frequency of the nonlinearly vibrating tube, when performing time-domain numerical simulations. Several methods have been used by researchers in this field, including straight time-domain evaluations of the zero-crossing frequency or a time-window adaptation of Rice's formula [13]:

$$\overline{f}_r(x,t) = \frac{1}{2\pi}\frac{\sigma_{\dot{Y}}(x,t;\tau)}{\sigma_Y(x,t;\tau)} \tag{5}$$

or our own technique, which is thoroughly explained in [10]. It is convenient to define dimensionless coupling coefficients in terms of the reduced velocity, which may be presented in the following form [1,14]:

$$C_m = \frac{M_F}{(1/2)\rho D^2 L} \quad ; \quad C_d(V_R) = \frac{D_F(V_R)}{(1/2)\rho DVL} \quad ; \quad C_k(V_R) = \frac{K_F(V_R)}{(1/2)\rho V^2 L} \tag{6}$$

Then, after modal projections, the fluid-elastic force field (4) leads to the following modal forces:

$$\left\{\mathcal{F}^F(t)\right\} = -\left[\mathcal{M}_F\right]\left\{\ddot{Q}\right\} - \left[\mathcal{D}_F(t)\right]\left\{\dot{Q}\right\} - \left[\mathcal{K}_F(t)\right]\left\{Q\right\} \tag{7}$$

where the terms of the modal fluid-elastic coupling matrices are computed as:

$$m_{nm}^F = \int_0^L M_F\varphi_n(x)\varphi_m(x)dx \quad ; \quad d_{nm}^F(t) = \int_0^L D_F\left(V_R(x,t)\right)\varphi_n(x)\varphi_m(x)dx \quad ; \quad k_{nm}^F(t) = \int_0^L K_F\left(V_R(x,t)\right)\varphi_n(x)\varphi_m(x)dx \tag{8}$$

From (2) and (7) one can obtain the changes in the system modal properties, due to the fluid-elastic coupling, as a function of the flow velocity. In the frequency domain:

$$\left[\lambda^2\left(\left[\mathcal{M}_S\right]+\left[\mathcal{M}_F\right]\right)+\lambda\left(\left[\mathcal{D}_S\right]+\left[\mathcal{D}_F(V_R)\right]\right)+\left(\left[\mathcal{K}_S\right]+\left[\mathcal{K}_F(V_R)\right]\right)\right]\left\{\overline{Q}\right\} = \left\{\mathbf{0}\right\} \tag{9}$$

where $\lambda_n(V_R) = \sigma_n(V_R) \pm i\,\nu_n(V_R)$ are the complex eigenvalues of the flow-coupled system, which are related to the modal properties as $\omega_n(V_R) = \sqrt{\sigma_n^2(V_R) + \nu_n^2(V_R)}$ and $\zeta_n(V_R) = -\sigma_n(V_R)/\omega_n(V_R)$. Notice that, because the modal coupling coefficients depend on the response frequencies encapsulated in V_R, the eigen-computation (9) should be performed in iterative manner.

Random buffeting Forces

Modeling of the turbulence excitation $f_T(x,t)$ by the transverse flow is based on the general theory developed by Axisa et al. [15]. Then, generation of time-domain realizations of the turbulence forces is achieved using the efficient method recently proposed by Antunes et al. [16]. Accordingly, we start from the measured equivalent reference spectrum $\left[\Phi\right]_e(f_R)$ of the random forces per unit tube length. Then, a set of uncorrelated random point forces is applied along the tube, using a computation technique which preserves the spectral content as well as the space correlation of the original turbulence force field, accounting for the flow velocity profile. See the aforementioned references for details.

As is well known, the random excitation data from single-phase flows collapse well when plotted in terms of the reduced frequency f_R and the force spectra are reduced using the square of the pressure head, see [15]. Unfortunately, the scenario is much more complex when working with two-phase flows, and finding satisfactory dimensionless parameters for two-phase buffeting excitation spectra still remains an open issue, because of the flow complexity and the complex manner in which the flow structure and buffeting forces depend on the flow velocity and on the void fraction, as discussed by Axisa et al. [15] and de Langre & Villard [17]. However, such problem is slightly alleviated in the present work, as shown in the following, because we are dealing here with a single value of the void fraction $\alpha = Q_{air}\big/\left(Q_{air} + Q_{liq}\right) = 0.85$, where Q_{air} and Q_{liq} are the volume flow rates of air and water, respectively.

Contact Forces at Loose Supports

A single nonlinear loose support is assumed in this paper, in accordance with the experimental rig. The contact force $F_C(t)$ is computed in an explicit manner from the system response, at each time-step, using the following penalty formulation:

$$F_C(t) = \begin{cases} -K_C\left[Y\left(x_C,t\right)-\delta_C\right] & \text{if} \quad \left|Y\left(x_C,t\right)\right| > \left|\delta_C\right| \\ 0 & \text{if} \quad \left|Y\left(x_C,t\right)\right| < \left|\delta_C\right| \end{cases} \tag{10}$$

where K_C is a suitable value for the contact stiffness at the support, which is pragmatically adjusted such that the numerical simulations reproduce the elementary contact duration of the experimental impacts. Because the tube motions studied in this paper are planar and the corresponding impacts only display a radial component, there is no need to implement a friction contact model [11].

EXPERIMENTAL RIG AND TEST PROCEDURES

The test rig, shown in Fig. 1, is essentially the one used in [9] in their tests, however a new instrumented tube with quite different modal frequency was used in the present experiments. Furthermore, the present experiments were designed for flow-excited vibro-impacting on an instrumented loose support. The flexible steel tube, with the previously stated length L_f and diameter D, has a thin wall $e = 0.5$ mm, being relatively light when compared with the added mass from the external fluid. The tube is clamped through a flat bar of length 100 mm, in order to constrain the vibrations to be planar. This tube is the central one of a 3×5 square bundle of rigid tubes with reduced pitch $P/D = 1.5$ (plus two columns of 5 half-tubes at the boundaries). The first modal frequency of the rigid tubes lay beyond 1 kHz, two orders of magnitude higher than the first modal frequency of the flexible tube. For illustration, the modeshapes of the first four modes of the flexible tube, based on a finite element computation, are shown in Fig. 2.

Two-phase air/water flows with void fraction $\alpha = 0.85$ were imposed along the vertical direction, with inter-tubes velocity in the range $V_h = 3 \sim 20$ m/s, based on the homogeneous flow model. Measurement of the tube dynamical displacement, along the lift (horizontal) direction, was provided by a Zimmer camera OHG-100A, pointed toward the end of the tube. As shown in Fig. 1, for the nonlinear tests, two instrumented gap-stops were located symmetrically at the tube half-length. The impact force measurements were performed by two piezoelectric force transducers Kistler 9132A.

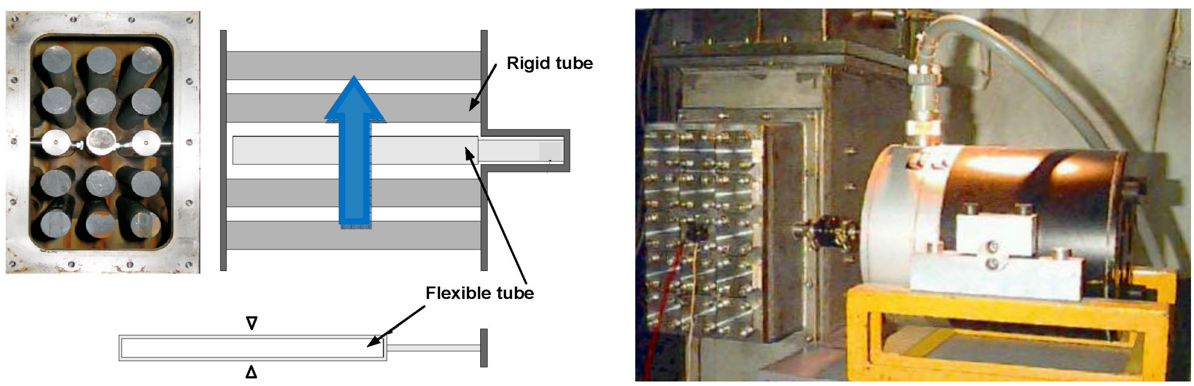

Fig.1: Experimental rig and electromagnetic shaker for feedback control of the tube damping and stabilization

The first tests, performed under linear conditions (no loose support), were intended for the experimental identification of the fluid-elastic coupling coefficients $C_d(V_R)$ and $C_k(V_R)$, the added mass C_m being assumed independent of the flow velocity. In order to explore the full range of experimental reduced velocity – beyond the fluid-elastic stability boundary of the "normal" system – the analog feedback stabilization technique [9] has been adopted. It is, essentially, the one used earlier by Antunes et al. [18] in their feedback controlled instability tests, but with reversed polarity. As implemented in the present experiments at CEA, the flexible tube was fitted with an accelerometer Endevco 2222C, located near the node of the tube second mode, whose response signal was electronically time-integrated and amplified, being then fed to the electromechanical shaker shown in Fig. 1.

A negative feedback loop was thus created, enabling a higher value of the tube first mode damping, which was controlled through the gain of the power amplifier. Note that, due to the filtering used in the feedback loop to avoid undue modal spillover, the control force was not exactly in phase with the tube velocity. As a result, some residual feedback also affected the stiffness term, resulting in a change of the controlled tube modal frequency. This effect was carefully corrected when extracting the flow-coupling coefficients from the identified modal parameters. This control system enabled us to identify the fluid-elastic coefficients under linear conditions in the range $V_h = 3 \sim 20$ m/s, corresponding to the reduced velocity $V_R = 3.5 \sim 17.5$.

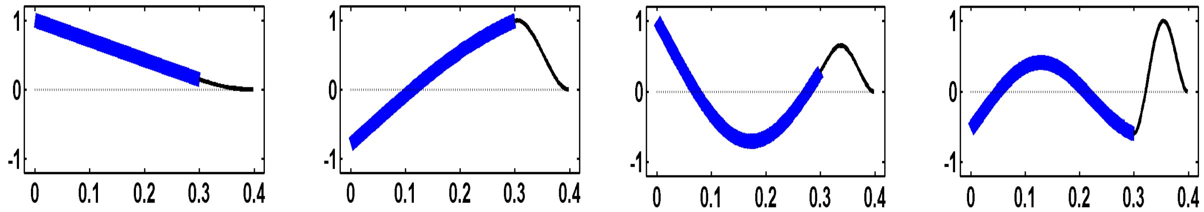

Fig.2: First modeshapes of the modal basis used for the nonlinear time-domain computations

FLUIDELASTIC AND BUFFETING FORCES FROM THE TRANSVERSE FLOW

Identified Fluid-Elastic Force Coefficients

Because the added mass C_m is assumed independent of the flow velocity, the inertia coupling by the flow is trivially obtained by comparing the modal frequencies in air and in "stagnant" fluid, respectively 31.0 Hz and 27.6 Hz for the first mode. Similarly, the viscous fluid damping coefficient $C_d(0)$ at near-zero flow velocity can be inferred from the modal damping values in air and in "stagnant" fluid, respectively 0.33 % and 5.0 %. The corresponding values of the modal mass, for the first mode, were found to be 0.066 kg and 0.071 kg (with modeshapes normalized such that $\max[|\varphi_n(0 \le x \le L)|] = 1$, as shown in Fig. 2).

Application of the general formulation (9) to our system has shown that the incidence of the fluid-elastic forces on the tube higher-order modes is negligible. Therefore, under flow conditions, the fluid-elastic coupling coefficients $C_k(V_R)$ and $C_d(V_R)$ are also easily inferred from the identified first modal frequency $f_1(V_R)$ and damping value $\zeta_1(V_R)$, accounting for the added damping from the stabilizing feedback loop – see [9] for details. The fluid-elastic coefficients, identified from the system response to the flow random excitation, are shown in Fig. 3 as a function of the reduced flow velocity V_R. In accordance with equation (7), the sign convention for the fluid-elastic coefficients plotted in Fig. 3 is such that positive values of $C_k(V_R)$ would increase the modal frequency of the flow/structure coupled system. Similarly, positive values of $C_d(V_R)$ are stabilizing. Notice that, for the full range of flow velocity explored in the tests, $C_k(V_R)$ is positive, changing with V_R in a capricious manner. More importantly, the general trend of $C_d(V_R)$ decreases as V_R increases, clearly becoming negative beyond $V_R > 14$, or equivalently $V_h = 13$ m/s. Then, accounting for the added damping term under "stagnant" conditions, fluid-elastic instability by negative damping arises beyond the critical reduced velocity $V_{RC} > 16$, or equivalently $V_{hC} = 16$ m/s. Also notice the local increase of C_d in the range $V_R \approx 10 \sim 12$, a behavior which might be attributed to a change of the flow regime.

Identified Turbulence Excitation

Using linear theory – see [14,15] for details – we identified the amplitude of the buffeting excitation spectrum from the random vibratory response of the tube first mode, as the flow velocity was increased. The dimensionless results thus obtained are shown in Fig. 4, as a function of the reduced frequency f_R. In the figure are shown the data points of the identified excitation at increasing flow velocity, as well as the corresponding dimensionless spectrum, fitted as:

$$[\Phi]_e(f_R) = \begin{cases} 4.32\,10^{-6}(f_R)^{-3.82} & \text{if} \quad f_R < 0.038 \\ 1.28\,10^{-2}(f_R)^{-1.39} & \text{if} \quad f_R \ge 0.038 \end{cases} \tag{11}$$

As previously discussed, it would hardly be straightforward to infer a relevant dimensionless two-phase spectrum if we were addressing a range of void fractions, instead of the single value $\alpha_h = 0.85$. Superimposed in the plot is the reference spectrum $[\Phi]_e(f_R)$ which was proposed as a design guideline by de Langre & Villard [17]. One can notice that, except at higher reduced frequencies, this guideline spectrum seriously overestimates the two-phase excitation identified for our experimental tube bundle, at this void fraction.

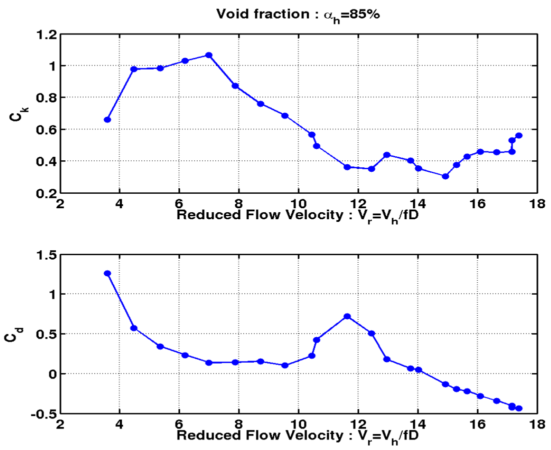

Fig.3: Identified dimensionless fluid-elastic coupling coefficients, as a function of the flow reduced homogeneous velocity, for the void fraction $\alpha_h = 0.85$

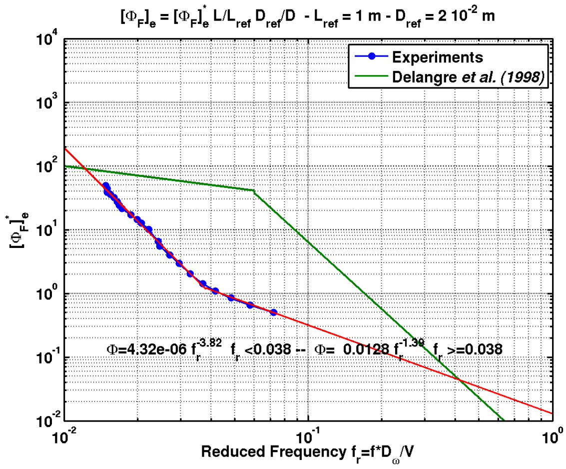

Fig.4: Identified excitation data at $\alpha_h = 0.85$, shown with the Equivalent Reference Spectrum of buffeting forces per unit length by de Langre & Villard [17]

COMPUTATIONAL AND EXPERIMENTAL VIBRO-IMPACT RESPONSES

We now address the most important aspect of this work, namely, the unsteady nonlinear dynamics of the vibro-impacting flow-excited tube. In Figs. 5 to 7 we present a comparison between the experimental and computational results, for the complete range of flow velocity explored, and for the two support gaps tested.

Figure 5 shows the average of the impact force maxima, a quantifier of the impact force magnitude. For $\delta_c = \pm 0.5$ mm, impacts are displayed by the system already at $V_h \approx 3$ m/s. However, for the larger gap $\delta_c = \pm 1$ mm, impacts only arise beyond $V_h \approx 4.5$ m/s. The impact forces magnitudes increase with the flow velocity in almost steady manner. The qualitative features of the experimental results are reproduced by the computations, including the velocity boundaries where the tube starts to impact. Quantitatively, the computed impact forces are quite satisfactory for the larger support gap, but overestimate (by up to 20 %) the corresponding experimental forces for the lower support gap. Notice that, at higher flow velocities, higher impact forces are observed on the larger-gap system. This is because the fluid-elastic forces are proportional to the system vibratory amplitude and hence, beyond instability, increase almost proportionally with δ_c.

In Fig. 6 we present the experimental and computational response frequencies of the system (both estimated according to Rice's formula) and, again, their comparison is highly satisfactory. The system experiences a steady increase of $\overline{f}_{Rice}$ with the flow velocity. This result is a direct consequence of an increase in the system effective stiffness, connected with increasingly intense vibro-impact dynamical regimes.

In Fig. 7 the average values of the reduced velocities obtained from the nonlinear experiments and computations are plotted as a function of the flow velocity. Recall that V_R only increases proportionally to V under linear conditions. For vibro-impacting systems this relationship is not straightforward, because the actual response frequency $\overline{f}_r$ used in $V_R = V / \overline{f}_r D$ is not constant, being dependent on the response regime of the nonlinear system. The dynamical behavior of gap-supported tubes subjected to fluid-elastic forces is clarified by Fig. 7, which shows the stabilizing effect of impacting on the dynamics of the linearly unstable tube.

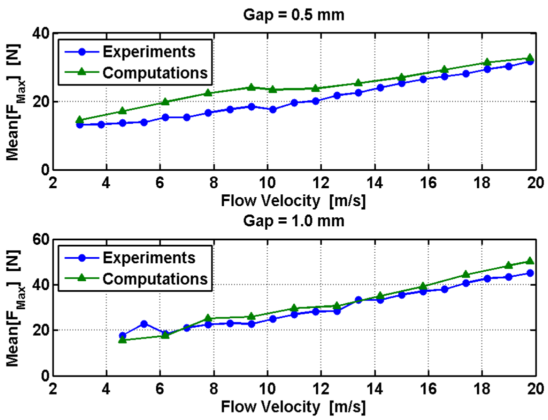

Fig.5: Comparison between the tube experimental and computed impact forces

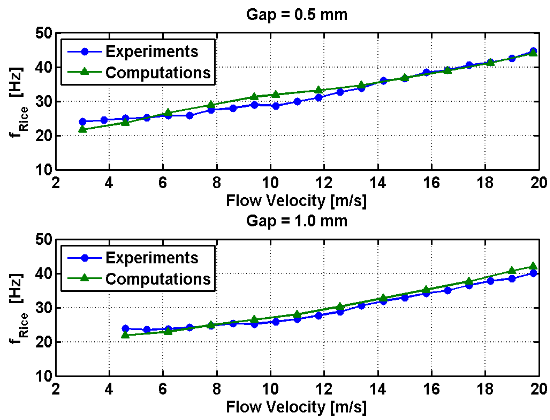

Fig.6: Comparison between the tube experimental and computed response frequencies

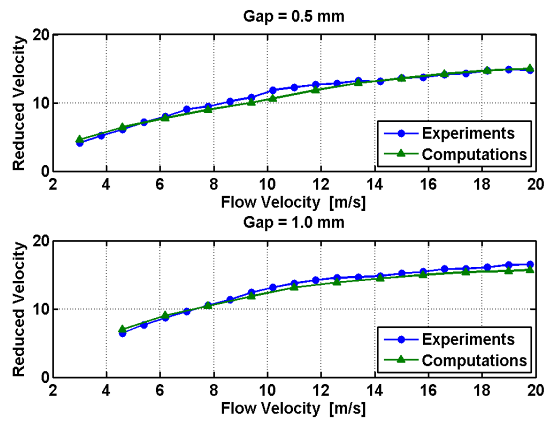

Fig.7: Comparison between the tube experimental and computed average reduced velocities as a function of the flow velocity

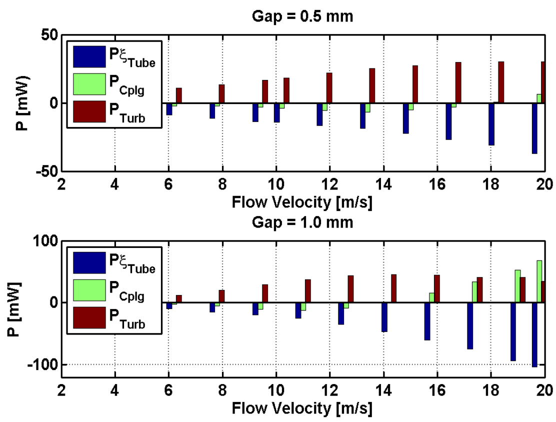

Fig.8: Computed power terms, pertaining to the tube damping, the flow coupling and turbulence, as a function of the flow velocity and support gap

Detailed information concerning the system energy balance is provided by the plots in Fig. 8. These were computed from the results of the numerical simulations, and quantify the power "flow-paths", for increasing values of the flow velocity and for the two support gaps addressed. Positive values indicate that energy is supplied to the tube, while negative values indicate dissipated energy. As expected, turbulence forces always supply energy and the structural damping is always dissipative. The most interesting part in these plots relates to the energy behavior stemming from the fluid-elastic coupling terms. Not surprisingly, these lead to unstable forces at higher flow velocities and are higher for the larger support gap.

CONCLUSIONS

In this paper we presented preliminary experimental and computational results which constitute an overall validation of our approach to deal with gap-supported tubes subjected to two-phase fluid-elastic forces and buffeting excitation, at least for the single void fraction of the tests performed. Under nonlinear conditions, extensive experiments and computations were performed, for a large range of flow velocity and two values of the tube support gap. The agreement between the nonlinear experimental and computational results (demonstrated in Figs. 5 to 7) enable us to conclude that it is satisfactory to use the fluid-elastic coefficients $C_k(V_R)$ and $C_d(V_R)$, obtained under steady linear conditions, for performing severely nonlinear unsteady computations. On the other hand, the analysis of the results provided by the two support gaps tested highlight the interesting scenarios which may arise, with respect to the various terms involved in a power balance of the flow-excited tube.

ACKNOWLEDGMENTS

The authors acknowledge financial support for this work, which was performed in the framework of a joint research program co-funded by AREVA NP, EDF and CEA (France). Also, concerning the experimental part of this paper, we gladly acknowledge the valuable contribution of THIERRY VALIN, from CEA/DEN/DM2S/SEMT/DYN (Saclay, France).

REFERENCES

[1] Tanaka, H., Takahara, S., "Fluidelastic Vibration of Tube Arrays in Cross-Flow", *Journal of Sound and Vibration*, Vol. 77, 1981, pp. 19-37.

[2] Connors, H.J., "Fluidelastic Vibration of Tube Arrays Excited by Cross-Flow", *Proc. Flow-Induced Vibration in Heat-Exchangers* (Reiff, D.D. Ed), ASME, 1970, pp. 42-46.

[3] Axisa, F., Antunes, J., Villard, B., "Overview of Numerical Methods for Predicting Flow-Induced Vibration", *ASME Journal of Pressure Vessel Technology*, Vol. 110, 1988, pp. 6-14.

[4] Fricker, A., "Numerical analysis of the fluid-elastic vibration of a steam generator tube with loose support", *Journal of Fluids and Structures*, Vol. 6, 1992, pp. 85-107.

[5] Rao, M.S., Steininger, D.A., Ahluwalia, K.S., Eisinger, F.L., "Simulation of PWR Steam Generator Tubes Undergoing Turbulence and Fluidelastic Excitation for Wear Prediction", *ASME International Symposium on Flow-Induced Vibrations and Noise*, Anaheim, USA, Vol. 230, 1992, pp. 185-210.

[6] Sauvé, R.G., "A Computational Time Domain Approach to Fluidelastic Instability for Nonlinear Tube Dynamics", *Symposium on Flow-Induced Vibrations*, Montreal, Canada, ASME PVP/ICPVT-8, 1996, pp. 111-121.

[7] Hadj-Sadok, C., Payen, T., de Langre, E., "Modelling of Fluidelastic Vibrations of Heat Exchanger Tubes with Loose Supports", *4th International Symposium on Fluid-Structure Interaction, Aeroelasticity and Flow-Induced Vibration and Noise*, Dallas, USA, 1997, Vol. 53-2, pp. 193-199.

[8] Hassan, M., Hayder, M., "Nonlinear Vibrations of Loosely Supported Tubes Excited by Fluidelastic and Turbulence Forces", *Nuclear Engineering and Design*, Vol. 238, 2008, pp. 2507-2520.

[9] Caillaud, S., de Langre, E., Piteau, P., "The Measurement of Fluidelastic Effects at Low Reduced Velocities Using Piezoelectric Actuators", *ASME Journal of Pressure Vessel Technology*, Vol. 121, 1999, pp. 232-238.

[10] Piteau, P., Delaune, X., Antunes, J., Borsoi, L., "Vibro-Impact Experiments and Computations of a Gap-Supported Tube Subjected to Single-Phase Fluid-Elastic Coupling Forces", *ASME 7th International Symposium on Fluid-Structure Interactions, Flow-Sound Interactions and Flow-Induced Vibration and Noise*, Montreal, Canada, 2010. To appear in *Journal of Fluids and Structures*, 2011.

[11] Antunes, J., Axisa, F., Beaufils, B., Guilbaud, D., "Coulomb Friction Modelling in Numerical Simulations of Vibration and Wear Work Rate of Multi-Span Heat-Exchangers", *Journal of Fluids and Structures*, Vol. 4, 1990, pp. 287-304.

[12] Lever, J.H, Weaver, D.S., "A Theoretical Model for the Fluidelastic Instability in Heat Exchanger Tube Bundles", *ASME Journal of Pressure Vessel Technology*, Vol. 104, 1982, pp. 147-158.

[13] Rice, S.O., "Mathematical Analysis of Random Noise", *Bell System Technical Journal*, Vol. 24, 1945, pp. 46-156.

[14] Granger, S., Campistron, R., Lebret, J., "Motion-Dependent Excitation Mechanisms in a Square In-Line Tube Bundle Subject to Water Cross-Flow: An Experimental Modal Analysis", *Journal of Fluids and Structures*, Vol. 7, 1993, pp. 521-550.

[15] Axisa, F., Antunes, J., Villard, B., "Random Excitation of Heat-Exchanger Tubes by Cross-Flow", *Journal of Fluids and Structures*, Vol. 4, 1990, pp. 321-341.

[16] Antunes, J., Delaune, X., Piteau, P., Borsoi, L., "A Simple Consistent Method for the Time-Domain Simulation of Turbulence Excitations Applied to Tube/Support Dynamical Analysis Under Non-Uniform Flows", *9th International Conference on Flow Induced Vibrations (FIV-2008)*, Prague, Czech Republic, 2008.

[17] de Langre, E., Villard, B., "An Upper Bound on Random Buffeting Forces Caused by Two-Phase Flows Across Tubes", *Journal of Fluids and Structures*, Vol. 12, 1998, pp. 1005-1023.

[18] Antunes, J., Axisa, F., Vento, M.A., "Experiments on Tube-Support Interaction with Feedback Controlled Instability", *ASME Journal of Pressure Vessel Technology*, Vol. 114, 1992, pp. 23-32, 1992.